Sterol preservation in hypersaline microbial mats

Yan Shen[1], Volker Thiel[1], Pablo Suarez-Gonzalez[2], Sebastiaan W. Rampen[1], Joachim Reitner[1,3]

[1]Department of Geobiology, Geoscience Centre, Georg-August-Universität Göttingen, Göttingen, Germany
[2]Área de Geología, Universidad Rey Juan Carlos, Madrid, Spain
5   [3]'Origin of Life' Group, Göttingen Academy of Sciences and Humanities, Göttingen, Germany

Correspondence to: Yan Shen (yshen@gwdg.de)

Abstract. Microbial mats are self-sustaining benthic ecosystems composed of highly diverse microbial communities. It has been proposed that microbial mats were widespread in Proterozoic marine environments, prior to the emergence of bioturbating organisms at the Precambrian-Cambrian transition. One characteristic feature of Precambrian biomarker records is that steranes are typically absent or occur in very low concentrations. This has been explained by low eukaryotic source inputs, or degradation of primary produced sterols in benthic microbial mats ("mat-seal effect"). To better understand the preservational pathways of sterols in microbial mats we analysed freely extractable and carbonate-bound sterols as well as decalcified extraction residues in different layers of a recent calcifying mat (~1500 years) from the hypersaline Lake 2 on the island of Kiritimati, Central Pacific. A variety of C_{27}-C_{29} sterols and distinctive C_{31} 4α-methylsterols (4α-methylgorgosterol and 4α-methylgorgostanol, biomarkers for dinoflagellates) were detected in both lipid pools. These sterols most likely originated from organisms living in the water column and the upper mat layers. This autochthonous biomass experienced progressive microbial transformation and degradation in the microbial mat, as reflected by a significant drop in total sterols concentrations, up to 98 %, in the deeper layers, and a concomitant decrease in total organic carbon. Carbonate-bound sterols were generally low in abundance, suggesting that incorporation into the mineral matrix does not play a major role for the preservation of eukaryotic sterols in this mat. Likewise, pyrolysis revealed that steroids (i.e., including sterenes, steranes and sterols), in contrast to hopanoids, were not sequestered into insoluble organic matter which may give rise to a further bias in the preservation of steroids vs. hopanoids, particularly in the later stages of burial. While these findings argue for a strong 'mat-seal effect' in the mat studied, they markedly differ from recent findings made for another microbial mat growing in the near-by hypersaline Lake 22 on the same island, where sterols showed no systematic decrease with depth. The observed discrepancies in the taphonomic pathways of sterols in microbial mats from Kiritimati may be linked to multiple biotic and abiotic factors including salinity and periods of subaerial exposure, implying that caution has to be exercised in the interpretation of sterols distributions in modern and ancient microbial mat settings.

1 Introduction

Sterols, biological precursors of steroids, are commonly used as biological markers for specific classes of organisms (Atwood et al., 2014; Brocks and Summons, 2004; Rampen et al., 2009; Volkman, 1986; Volkman, 2005). Sterols have been found in many different types of depositional environments such as soils (van Bergen et al., 1997; Birk et al., 2012; Otto and

5 Simpson, 2005), recent lacustrine and marine sediments (Brassell and Eglinton, 1983; Gaskell and Eglinton, 1976; Robinson et al., 1984; Volkman, 1986), as well as microbial mats from meso- to hypersaline conditions (Grimalt et al., 1992; Scherf and Rullkötter, 2009). Further, the hydrocarbon skeleton of sterols is relatively stable, and thus significant amounts can be preserved in the geological record (Brocks et al., 2017; Mattern et al., 1970).

Microbial mats are vertically laminated organo-sedimentary structures, which are primarily self-sustaining ecosystems

10 (Des Marais, 2003), ranging in thickness from millimeters to decimeters. The mineralized fossil product of microbial mats are microbialites, which have a long geological history of over 3 billion years, indicating that microbial mats probably represented the earliest complex ecosystems on Earth (Reitner and Thiel, 2011). Microbial mats typically consist of many different functional groups of microorganisms which control the organic matter (OM) turnover in the microbial mat. Major groups include cyanobacteria, colorless sulfur bacteria, purple sulfur bacteria and sulfate-reducing bacteria, but also

15 eukaryotic organisms (Schneider et al., 2013; van Gemerden, 1993). A large proportion of the OM consists of extracellular polymeric substances (EPS), secreted by the microorganisms, which are crucial for the support and the development of the microbial mat (Wingender et al., 1999; Decho, 2011; Reitner and Thiel, 2011). EPS are rich in acidic groups that bind cations such as Ca^{2+}, thereby inducing a strong inhibitory effect on the precipitation of common minerals formed within microbial mats, such as $CaCO_3$ (Arp et al., 1999; Dupraz et al., 2009; Ionescu et al., 2015). Consequently, carbonate

20 precipitation often occurs in deeper and older mat layers in which decomposing EPS gradually releases previously-bound Ca^{2+}, thus facilitating carbonate supersaturation (Arp et al., 1999; Dupraz et al., 2009; Ionescu et al., 2015). Previous studies indicate that early sequestration into a mineral matrix may promote the preservation of organic compounds (Summons et al., 2013; Smrzka et al., 2017; Thiel et al., 1999). Hence, microbial mats possibly provide an enhanced chance for OM to survive in the geosphere if carbonate or other mineral precipitation occurs therein.

25 In the Proterozoic, microbial mats have been proposed to be a predominant life form in marine environments, in contrast to the Phanerozoic that is characterized by prosperity of biota (including fauna and flora) and a low abundance of benthic microbial mats (Grotzinger and Knoll, 1999; Riding, 2011; Walter, 1976). One of the characteristic features of the Precambrian biomarker records is that eukaryotic steranes are typically absent or occur in very low concentrations. This may be explained by a limited ecological distribution of eukaryotic algae and thus minor contributions of sterols to sedimentary

30 OM (Anbar and Knoll, 2002; Blumenberg et al., 2012; Brocks et al., 2017; Knoll et al., 2007), and/or by a thermal degradation of sterols during catagenesis (e.g. in the 1640 Ma Barney Creek Formation and 1430 Ma Velkerri Formation, Northern Australia, Dutkiewicz et al., 2003; Summons et al., 1988). An alternative explanation would be that eukaryotic lipids have been subject to a preservation bias due to the ubiquity of benthic microbial mats. It has been hypothesized that

these mats would have formed a significant mechanical and chemical barrier against the preservation of eukaryotic lipids sourced from water column and upper mat layers, a phenomenon termed as "mat-seal effect" (Pawlowska et al., 2013). Selective preservation induced by the mat-seal effect would also impart a bias in favour of lipids derived from heterotrophic microorganisms living in the deeper mat layers, and cause a suppression of the primary ecological signal. This is different

5   from the situation in the Phanerozoic, where OM from planktonic primary producers (including algae and bacteria) is more rapidly transferred to the sediment through sinking aggregates (such as crustacean faecal pellets), and without being reworked in benthic microbial mats (Close et al., 2011; Fowler and Knauer, 1986; Logan et al., 1995).

The Kiritimati atoll (Kiribati Republic, Central Pacific, Fig. 1) is an ideal study site for investigating the taphonomy of sterols in microbial mats. The island is covered by c. 500 brackish to hypersaline lakes, most of which are populated by thick

10   and highly developed benthic mats that are clearly laminated and show ongoing mineral precipitation, i.e. microbialite formation (Arp et al., 2012; Trichet et al., 2001; Valencia, 1977). Therefore, Kiritimati enables studies on the behaviour of sterols within various types of microbial mats thriving under different environmental conditions and showing different degrees of mineralization.

A recent study conducted on a microbial mat from Lake 22 on Kiritimati demonstrated that a range of sterols were

15   abundantly present in all parts of that mat. The lack of any systematic decrease with depth suggested that the sterols in that particular mat had not been impacted by a major mat-seal effect (Shen et al., 2018a). On the other hand, an earlier study on insoluble OM obtained from a microbial mat from a different lake of the same island (Lake 2, located about 10 km south of Lake 22) reported an increasing trend of hopane/sterane ratios with depth (Blumenberg et al., 2015). In conjunction with other findings, this was considered indicative of a "*suppression of biosignatures derived from the upper mat layers*" and

20   thus, a mat-seal effect (Blumenberg et al., 2015). Since that work had a different focus and did not report detailed sterol data, it is not directly comparable with the results on the Lake 22 mat reported by Shen et al. (2018a). Therefore we revisited the microbial mat from Lake 2 and performed a detailed analysis of sterol compounds, investigating both freely extractable as well as carbonate-bound lipid fractions, and also decalcified extraction residues. Our study was aimed at further examining general trends in the preservation of sterols in hypersaline microbial mat systems by comparing the results from different

25   settings within the same geological and geographical context (i.e. Lakes 2 and 22).

2 Materials and methods

2.1 Location and samples

The atoll of Kiritimati (Republic of Kiribati) is located in the central part of the Pacific Ocean, close to the Equator (Fig. 1). Its surface displays a complex reticular pattern encompassing c. 500 lakes with salinities that range from brackish to

30   hypersaline. Most of the lakes harbour thick microbial mats that show ongoing mineralization processes (Figs. 1, 2) and generally occur on top of older, more developed microbialites (i.e. already fossilized microbial mats; Arp et al., 2012; Ionescu et al., 2015; Trichet et al., 2001; Valencia, 1977). Vegetation around the lake areas comprises the mangrove

Rhizophoramucronata, the parasitic climber *Cassytha filiformis*, the grass *Lepturus repens*, and the ironwood *Pemphis acidula* (Fig. 2e; Saenger et al., 2006). The climate of Kiritimati is broadly controlled by the El Niño-Southern Oscillation (ENSO) atmospheric phenomenon. During El Niño wet events, heavy rains occur, decreasing lake salinities; whereas reduced precipitation during La Niña dry events triggers higher evaporation and increasing lake salinities (Arp et al., 2012;

5 Saenger et al., 2006; Trichet et al., 2001). Materials studied in this work were sampled from Lake 2 (Fig. 1), whose salinity was 97 ‰ in 2002 and 125 ‰ in 2011 (own data, unpublished). This high and variable salinity causes low metazoan diversity within Lake 2. Faunal elements include abundant *Tilapia* fish (Fig. 2d) and *Artemia* brine shrimp as well as few land crabs, and unicellular miliolid foraminifera (Saenger et al., 2006; Shen et al., 2018a). Events of mass mortality of fish have been observed in some of the lakes (Fig. 2d), which may be linked to extreme hypersaline conditions probably due to

10 heavy evaporation during La Niña dry periods. More detailed information about the environmental setting of Kiritimati can be found elsewhere (Arp et al., 2012; Saenger et al., 2006; Shen et al., 2018a; Trichet et al., 2001).

In this work, a microbial mat from the hypersaline Lake 2, previously studied by Blumenberg et al. (2015), was analysed for sterols (Fig. 1). This mat is 10 cm thick and was sampled from the centre of the lake (water depth c. 4 m) during a field campaign in March 2011 (Figs. 1, 2). Samples were stored at -20°C until laboratory preparation. Based on the macroscopic

15 appearance, Blumenberg et al. (2015) divided the mat in five layers, the topmost layer corresponding to the photosynthetically active mat, and layers 2-5 representing ancient mat generations being degraded by recent anaerobic microorganisms (Figs. 1, 2). For this study, we used the same layer division as Blumenberg et al. (2015). However, a thin but distinctive mineral crust occurring just below layer 2 (Fig. 2c) has not been analysed in the previous study and is additionally included here (corresponding to our layer 3, Figs. 1, 2). Therefore, six layers in total were analysed in this work, each one c.

20 1-2 cm thick (except layer 3 ~0.15 cm).

2.2 Bulk analysis

Homogenized (mortar) aliquots of the freeze-dried samples (both original mat layers and extraction residues) were subjected to C/N/S analysis, using a Hekatech EA 3000 CNS analyzer and LECO RC 612 multiphase carbon analyser as described elsewhere (Shen et al., 2018a).

25 ## 2.3 Extraction and derivatization

Aliquots of the freeze-dried samples (5-20 g) were homogenized and extracted using 4×50 ml portions of dichloromethane/methanol (3:1; V/V) (10 min ultrasonication) to obtain the freely extractable lipids. The remaining extraction residues were decalcified using 37 % HCl (dropwise until CO_2 development ceased), and again extracted as described above to yield the carbonate-bound lipids. The remaining extraction residues (after decalcification) were freeze

30 dried for the analysis of bulk C_{org} and pyrolysis.

To make alcohols (including sterols) GC-amenable, aliquots of the lipid extracts (both freely extractable and carbonate-bound lipid fractions) were silylated using BSTFA (N,O-bis(trimethylsilyl)trifluoroacetamide) containing 5 % (V/V)

trimethylchlorosilane (TMCS) as a catalyser (70°C, 60 min). The resulting trimethylsilyl (TMS-) derivatives were dried under gentle N_2 flow, re-dissolved in *n*-hexane, and analysed by gas chromatography-mass spectrometry (GC-MS).

To make fatty acids GC-amenable, a mixture of TMCS/MeOH (1:9, V:V) was added to all aliquots of lipid extracts and samples were heated at 80°C for 60 min. The resulting fatty acid methyl esters were extracted from the reaction mixture by

5   vigorous shaking with 3×1 ml *n*-hexane. The extracts were combined and evaporated to near-dryness under a gentle stream of N_2, re-dissolved in *n*-hexane, and analysed by gas chromatography-mass spectrometry (GC-MS).

2.4 GC-MS

GC-MS analyses were carried out using a Thermo Fisher Trace 1310 GC coupled to a Thermo Fisher Quantum XLS Ultra MS as described elsewhere (Shen et al., 2018a). Due to low sterol concentrations and co-elutions, particularly in the deeper

10   mat layers, sterols were not quantified via peak integration in the total ion currents (TIC). Instead, the summed ion traces of $[m/z\ 129 + (M^+-90) + M^+]$ for the TMS-derivatives of Δ^5- and $\Delta^{5,22}$-stenols, and $[m/z\ 215 + (M^+-90) + M^+]$ for the TMS-derivatives of stanols were used. Appropriate correction factors were applied according to the response of these ions *vs.* concentration in the mass spectra of standard compounds. Average standard deviations of sterol concentrations were determined from repeated analyses of sample material.

15   ### 2.5 Pyrolysis-gas chromatography-mass spectrometry (Py-GC-MS)

Aliquots of the decalcified extraction residues were pyrolysed on a fast-heating Pt-filament using a Pyrola 2000 pyrolysis device (Pyrolab SB) coupled to a Varian CP3800 GC and a Varian 1200L MS as described elsewhere (Shen et al., 2018a).

2.6 Compound-specific stable carbon isotopes analysis

Compound-specific stable carbon isotope ratios were measured for sterols and fatty acids in the freely extractable lipid

20   fractions of the microbial mat. Analyses were conducted using a Thermo Scientific Trace gas chromatograph (GC) coupled to a Delta Plus isotope ratio mass spectrometer (IRMS). The conventional CuO/NiO/Pt reactor was used and combusted at 940°C. The GC-column used was an Agilent DB-5 coupled to an Agilent DB-1 (each 30 m length, 250 µm internal diameter, and 0.25 µm film thickness). Lipid fractions were injected into a splitless injector and transferred to the GC column at 290°C. The carrier gas was helium at a flow rate of 1.2 ml/min. The temperature program for analyzing lipid fractions was

25   ramped from 80°C, followed by heating to 325°C (at 5°C/min, held for 60 min). Analysis of laboratory standards were carried out to control the reproducibility of measuring conditions and measurements were calibrated by using CO_2 gas of known isotopic composition.

3 Results

3.1 General characterization of the microbial mat

The microbial mat has a thickness of c.10 cm. Based on its macroscopic appearance it shows two major phases of development. The upper, younger growth phase is represented by layer 1 (photosynthetically active mat) and layer 2 (each c.

5   1 cm thick, Figs. 1, 2). These layers have a cohesive texture, sticking together when handled, due to abundant and relatively fresh organic material (i.e. EPS) of bright orange, green and brown colours. Layer 1 includes small and scarce mineral precipitates, whereas layer 2 shows more abundant whitish minerals within its organic matrix (Fig. 2c). Layer 2 is underlain by a thin but distinctive, laterally continuous mineral crust (layer 3). Below the crust, layers 4, 5 and 6 (c. 7 cm thick in total, Figs. 1, 2) are more friable, having a crumbly appearance, due to a higher abundance of mineral particles as compared to

10 EPS. In this older growth phase, brown and beige colours predominate (Fig. 2c). The minerals observed within the mat layers are mainly aragonite ($CaCO_3$), with minor amounts of gypsum ($CaSO_4$) found only in the uppermost layer 1 (Shen et al., 2018b). Previously reported ^{14}C ages of the mat (Blumenberg et al., 2015) show that its upper growth phase formed in approximately 1000 years (62±40 years BP for layer 1, 551±40 years BP for layer 2 and 1111±40 years BP for layer 3; Fig. 1b) whereas the older (and thicker) growth phase formed approximately in the preceding 300 years (1331±40 years BP for

15 layer 5 and 1440±40 years BP for layer 6; Fig. 1b).

3.2 Bulk geochemical data

Bulk geochemical data for individual mat layers are shown in Table 1a. In the original mat (i.e. bulk sample before decalcification) relatively high C_{org} contents were observed in layers 1 and 2 (4.7 and 6.2 %, respectively; Table 1a and Fig. 3a), consistent with a more fresh, cohesive appearance of the organic matrix in these layers. Below layer 2, the earlier growth

20 phase consistently showed low and constant C_{org} contents < 2 %, with the lowest value found for layer 6 (1.2 %) (see 3.1). The $CaCO_3$ content of the mat increased significantly with depth (Fig. 3a; Table 1a). The lowest value was observed in the top layer 1 (27.1 %), a strong enrichment occurred in layer 2 (73.1 %), and constantly high contents > 90 % were found for all deeper mat layers. This is consistent with the observation of more abundant mineral precipitates downwards in the mat. The highest S content was detected for layer 1 (9.8 %), due to gypsum precipitates. Below, S decreased sharply (1.2 % in

25 layer 2) and retained low values (< 1 %) in the earlier growth phase of the mat (~0.3-0.5 %). N showed generally low contents (0.14-0.75 %) throughout the mat.

In the decalcified extraction residues (i.e., extraction residues after decalcification; Table 1b), C_{org} showed a broad range but increased significantly with depth, with the highest value observed in layer 6 (42.3 %; also see Fig. 3b). N was likewise enhanced in the deeper parts, with the highest amount found in layer 5 (6.7 %). By contrast, a decrease in S content was

30 observed with depth, with highest values occurring in the topmost mat layer 1 (10.4 %).

3.3 Sterol distributions and concentrations

Various sterols were detected within the mat, including saturated sterols (stanols; $C_{27}\Delta^0$, $C_{28}\Delta^0$, $C_{29}\Delta^0$, $C_{31}\Delta^0$) and unsaturated sterols (stenols; $C_{27}\Delta^5$, $C_{28}\Delta^{5,22}$, $C_{28}\Delta^5$, $C_{29}\Delta^{5,22}$, $C_{29}\Delta^5$, $C_{31}\Delta^5$, see Fig. 4; Table 2). Based on the retention characteristics and comparison with published mass spectra (Atwood et al., 2014; Houle et al., In Press), the C_{31} sterols were identified as

5   22,23-methylene-4α,23,24-trimethylcholest-5-en-3β-ol (4α-methylgorgosterol) and 22,23-methylene-4α,23,24-trimethylcholestan-3β-ol (4α-methylgorgostanol), respectively (see Fig. S1).

In the freely extractable lipids, stenols were by about an order more abundant than stanols. Both groups showed highest concentrations in layer 1, and a major decrease with depth (see Table 2a). Figure 5a shows the variations of C_{27}-C_{29} sterols (e.g. stenols *vs.* stanols) in the freely extractable lipids through the mat profile. The highest abundance of sterols occurred in

10   the topmost layer 1 (26.05 µg/g dry mat, see Fig. 5a). Concentrations decreased drastically in the upper layers, and remained low from layer 3 onwards. C_{28} and C_{29} sterols were the most dominant sterols in layer 1 while the C_{31} sterols dominated in the deeper layers (Fig. S3). The C_{31}-sterol distributions differed from the other sterol distributions identified in this mat, with concentrations in layer 5 being three to ten times higher than in layers 3, 4 and 6 (Fig. 3c; Table 2a). Further, in the freely extractable lipids, the ratios of 5α-stanols to their corresponding Δ^5-stenols (stanol/stenol ratios) showed no consistent trend

15   within the profile (Fig. 6a; Table 3). As expected, the C_{27}-, C_{28}- and C_{29}- ratios increased in the upper, younger growth phase of the mat, with the highest value observed for layer 3, but decreased again in the deeper, older growth phase (Fig. 6; Table 3). In contrast, stanol/stenol ratios for the C_{31} sterol declined from layer 1 to layer 5, and showed a remarkable increase in layer 6.

Sterol concentrations in the carbonate-bound lipid fractions are given in Table 2b. In the topmost layer 1, no carbonate-

20   bound sterols were observed. In mat layers 2 and 3, carbonate-bound sterols occurred, but were still much less abundant as freely extractable sterols (below detection limit to ~10^{-2} µg/g dry mat). In the deeper mat layers (4-6), however, sterols showed similar absolute concentrations (~10^{-2} - 10^{-3} µg/g dry mat) in both, the carbonate-bound and the freely extractable fractions. Sterenes were also detected in both lipid pools, but only at trace abundances (not discussed further).

In the carbonate-bound lipids, stenols comprised the predominant portion (c. from 65 % up to 90 % of all sterols) (Fig.

25   5b). Overall low abundances of carbonate-bound sterols were observed throughout the mat (10^{-1} µg/g dry mat range). C_{31}-groups were the primary contributors in both lipid fractions (ranging up to ca. 85 % in the deeper part of the mat), and C_{29}-groups were the second major inputs (Fig. S3). Carbonate-bound C_{31}-sterols increased in the bottom layer 6, which is distinguished from the other sterols (Fig. 3d). The stanol/stenol ratios in the carbonate-bound lipids, increased for the C_{27}-, C_{28}- and C_{29}- pairs between layers 1 and 3, and again decreased downwards as they did in the freely extractable lipids (see

30   Fig. 6b; Table 3). No stanol/stenol ratios could be obtained for the carbonate-bound C_{31} sterols, as C_{31} stenols were virtually absent throughout the mat.

3.4 Pyrolysis

Ion chromatograms representing steroids (i.e., including sterenes, steranes and sterols) and hopanoids released by pyrolysis of the decalcified extraction residues are shown in Fig. S2. Steroids were not observed in the pyrolysates throughout the mat, while hopanoids were found in the insoluble matter of each mat layer. Notably, only small amounts of hopanoid moieties

5   were observed in the pyrolysates of layer 1, but their abundance gradually increased with depth.

3.5 Compound-specific $\delta^{13}C$ values

A reliable compound-specific $\delta^{13}C$ value could be obtained for the coeluting C_{31}-sterols from the freely extractable lipids in layer 1. This compound showed a strong enrichment in ^{13}C ($\delta^{13}C$ = -7.2 ‰). Fatty acids (including C_{14}-C_{19} homologues) showed similarly high $\delta^{13}C$ values ranging from -4.4 to -11.7 ‰.

10   ## 4 Discussion

4.1 Biological sources of sterols

The studied mat contained a broad variety of C_{27}-C_{29} sterols as well as two C_{31} sterols, indicating potential sources like animals (C_{27}), fungi (C_{28}), algae including dinoflagellates (C_{27}-C_{29} + C_{31}) and terrestrial plants (C_{29}) (Atwood et al., 2014; Houle et al., In Press; Volkman, 1986; Volkman, 2003). The concentrations of freely extractable sterols in the topmost layer

15   1 in the studied Lake 2 mat are similar to Lake 2A and Lake 22 (~10^2-10^3 µg/g $C_{org;}$ Bühring et al., 2009; Shen et al., 2018a; see Fig. 5a). However, sterols in the deeper layers are much less abundant in the Lake 2 mat as compared to other mats in Kiritimati lakes.

   Figure S3 shows the relative distribution of summed C_{27}- vs. C_{28}- vs. C_{29}- vs. C_{31}- sterols in the microbial mat layers. In both lipid fractions, the C_{31}-sterols are predominant, suggesting inputs from dinoflagellates (Atwood et al., 2014; Houle et

20   al., In Press). C_{29}-sterols make up the next most abundant group, potentially indicating contributions from either algae or terrestrial plants (Volkman, 1986); also these compounds are known to be produced by diatoms and other algal groups (Rampen et al., 2010; Volkman, 2003).

   The high $\delta^{13}C$ value of -7.2 ‰ for the C_{31}-sterols, and similarly high values for the fatty acids measured from layer 1, imply that the carbon source of these compounds was autochthonous and derived from the hypersaline, CO_2-limited

25   ecosystem of Lake 2 (cf. Schouten et al., 2001). Previous work on carbon isotope compositions of sterols in a mat from the adjacent Kiritimati Lake 2A showed $\delta^{13}C$ values from -19 to -23 ‰ (Bühring et al., 2009). In addition, Trichet et al. (2001) reported $\delta^{13}C$ values for sedimentary bulk OM from -14 to -17 ‰ in Kiritimati Lake 30. Both studies showed more depleted values than those observed for Lake 2. An explanation could be a better CO_2 exchange in those lakes, due to their shallow water layer (a maximum depth of 0.2 m in Lake 2A, Bühring et al., 2009; depth of 0.9 m in Lake 30, Trichet et al., 2001),

30   leading to the relatively light $\delta^{13}C$ signatures. Another explanation could be that shrinking lake water bodies caused by La

Niña dry events are often associated with massive increases in lake salinities (Trichet et al., 2001). For instance, Lake 2A (Bühring et al., 2009) was observed to be nearly dried out during our sampling campaign in 2011. The increasing salinities may result in a CO_2-limited ecosystem, leading to enrichment in ^{13}C. The resulting reinforced CO_2-limitation in Lake 2 is not only reflected by the high $\delta^{13}C$ values of sterols and fatty acids in this work, but also $\delta^{13}C$ values of carbonates that were

5   observed to be as high as +6 ‰ (Arp et al., 2012).

4.2 Taphonomy of sterols

The sterols in the studied mat are probably sourced from plankton or organisms thriving at the mat surface, because eukaryotes are generally depending on an oxygenated environment and would hardly thrive in anoxic, deeper parts of the mat. It can also be expected that sterols were initially introduced as stenols. Subsequent alteration by early diagenetic

10   processes within the mat would have resulted in a variety of sterol transformation products. Reduction of Δ^5-stenols to 5α-stanols (hydrogenation) is a known result of anaerobic microbial degradation (Rosenfeld and Hellman, 1971; Wakeham, 1989). Consequently, stanol/stenol ratios may reflect the extent of microbial stenol alteration under anoxic conditions (i.e. under low redox potential; Gaskell and Eglinton, 1975; Nishimura, 1977; Wakeham, 1989). Several investigations have reported such conversion in microbial mats (Grimalt et al., 1992; Scherf and Rullkötter, 2009; Słowakiewicz et al., 2016),

15   including some mats from other lakes on Kiritimati (Bühring et al., 2009; Shen et al., 2018a).

In the mat studied, stanol/stenol ratios for C_{27}-C_{29} pairs initially increased with depth and showed highest values in layer 3, suggesting low redox potentials and a pronounced anaerobic microbial transformation of stenols therein. In the deeper layers (4-6), ratios decreased again. We interpret this to result from a more efficient microbial OM degradation, which occurred under higher redox potentials during the more rapid accretion of the earlier growth phase of the mat (1440-1111

20   years BP, see Fig. 1b). This idea is supported by constantly lower C_{org} contents in the earlier growth phase of the mat (1.20-1.47 %, see Table 1a). Exclusively for the C_{31}-stanol/stenol ratios, they showed a steady decrease with depth but sharply increased again in the bottom layer 6. It could be possible that input variations of the C_{31} stanol and stenol played a more important role than microbial alteration for the distributions of C_{31} sterols. 4α-methylgorgostanol has been reported in a few dinoflagellate species belonging to the genera *Peridinium*, *Alexandrium* and *Pyrodinium*, (Atwood et al., 2014; Houle et al.,

25   In Press, and refs therein), and the mass spectra of the sterol we tentatively identified as 4α-methylgorgosterol is similar to that reported for a sterol occurring in resting cysts but not in the motile cells of the dinoflagellate *Peridinium umbonatum* var. *inaequale* (Amo et al., 2010). As a result, C_{31} sterols could partly have been derived from sedimentary resting cysts that may have been less affected by degradation during transport or microbial recycling than conventional C_{27}-C_{29} sterols. It may also be speculated that the unusual side-chain structure and methylation pattern of 4α-methylgorgosterols hamper enzymatic

30   microbial degradation (e.g. Giner et al., 2003, and refs therein). The steadily increasing relative abundances of C_{31}- *vs.* C_{27}-C_{29} sterols in the mat profile (Fig. S3) suggest that C_{31} sterols experienced different degradation patterns as compared to conventional sterols.

For the total sterols, concentrations of freely extractable sterols were high in the top layer but dropped sharply immediately below and kept at very low concentrations throughout the deeper mat (< 1 µg/g dry mat). Carbonate-bound sterols, on the other hand, were hardly detectable at the top of the mat, and likewise showed constantly low abundances below. These observations suggest that (i) freely extractable sterols are rapidly degraded in the upper layers of the mat and (ii) the carbonate matrix played no important role in encasing (i.e., preserving) sterols in this mat. This is in agreement with previous reports about minor amounts of such sterols in methane seep microbialites and ooids (Birgel et al., 2006; Thiel et al., 1999; Thiel et al., 2001; Summons et al., 2013). However, in those settings, high concentrations of microbial lipids preserved in the carbonate matrix possibly reflect a constructive role of their source organisms in carbonate formation and/or their continuous incorporation into carbonate during the precipitation processes (Summons et al., 2013; O'Reilly et al., 2017). For instance, abundant ^{13}C-depleted acyclic isoprenoids encased in ancient methane-derived carbonates have been shown to originate from methane-oxidizing archaea whose metabolism immediately enhanced calcification (Peckmann and Thiel, 2004).

Blumenberg et al. (2015) pointed out that organic compounds in the deeper parts of the Lake 2 mat, unlike those at the top, are better preserved in the insoluble OM fraction, which is concordant with the results in this work (Fig. 2S). Specifically, our pyrolysis of the decalcified extraction residues revealed that steroids were not sequestered into insoluble OM, while hopanoids were present in all mat layers (Fig. S2). This phenomenon was also observed for pyrolysates in Lake 22 mat (Shen et al., 2018a). An explanation could be that the low number of reactive sites in common sterols (i.e. one hydroxyl-group) would lead to a low tendency to incorporate into macromolecular OM as compared to hopanoids (e.g. highly functionalized bacteriohopanepolyols with several hydroxyl-groups). This behaviour may eventually give rise to a further preservational bias of steroids vs hopanoids over geological time.

In the Lake 2 mat studied here, the strong decline in freely extractable sterols below the uppermost mat layer, along with the lack of any significant carbonate incorporation, suggests major degradation of steroids vs. hopanoids during early diagenesis (i.e. on a timescale of 10^2-10^3 years).

4.3 Comparison with sterol taphonomy in other microbial mats

The results from the Lake 2 mat differ significantly from the results of a previous study on a microbial mat profile in another lake in Kiritimati (Lake 22; Shen et al., 2018a). Sterol concentrations from the topmost layers are similar in both mats (10^2 µg/g C_{org} range), but the Lake 22 mat showed no systematic decrease in sterols with depth. Such entirely different behaviour of sterols in these two lakes raises questions about potential mechanisms causing the observed variation.

One explanation for the differences between the Lake 2 and 22 mats could be variations in salinity. In 2011, the salinity of Lake 22 (Shen et al., 2018a) was 250 ‰, whereas Lake 2 showed 125 ‰. High salinity may reduce microbial cell growth and reproduction, and limit the metabolism of microorganisms. The resulting decrease in bacterial activity would affect the biodegradation rates of organic compounds (Abed et al., 2006). Several studies reported that the degradation rates of hydrocarbons significantly decrease as salinity increases (microbial mat from Saudi Arabia, Abed et al., 2006; water and tar

samples from Great Salt Lake, Ward and Brock, 1978). On the other hand, lower salinity supports the proliferation of a more diverse microbial community (Bolhuis et al., 2014), thus possibly enhancing OM biodegradation. As a consequence, conditions for mat-forming microorganisms would be more favourable in Lake 2 as compared to the extremely hypersaline Lake 22, thus accelerating the biodegradation rates of organic molecules, including sterols. Another possible reason might be

5 decreased precipitation resulting in the decline of water depth. A major drought period prevailed in Kiritimati from 2002 to 2011, as a result of a very strong La Niña dry event. Due to reduced rainfall, the water level of the lakes in Kiritimati generally dropped, so that, in some areas, parts of the lake bottoms became subaerially exposed. The Lake 22 microbial mat was collected at the margin of the lake (Fig. 2f; water depth c. 0.2 m; Shen et al., 2018a). Therefore, mats from this shallow sampling site may have suffered from heavy evaporation due to such major drought events. As pointed out by Shen et al.

10 (2018a), the Lake 22 mat shows an irregular top layer of V-shaped fractures, which are general characteristic features of evaporitic settings, thus further demonstrating the repeated occurrence of dry periods in the region. On the other hand, the Lake 2 mat was collected in the lake centre (water depth c. 4 m) which is clearly less prone to subaerial exposure. These interpretations are further supported by other studies that highlighted how environmental conditions such as water depth and salinity may have a significant influence on the microbial composition of microbial mats (Pagès et al., 2014). In addition to

15 these environmental conditions, the differences of stanol/stenol ratios between the two lakes are noteworthy. Much higher ratios were observed in Lake 22 mat (Shen et al., 2018a), indicating a much more intense anaerobic microbial transformation (yet no degradation) as compared to the Lake 2 mat (Fig. 6). Whereas sterols in Lake 22 mat experienced major microbial *transformation* (stenols => stanols => sterenes), sterols in Lake 2 apparently suffered from major *degradation* that suppressed the primary ecological signal. The contrasting distributions observed for the Kiritimati mats studied also suggest

20 that sterols have a higher preservation potential in microbial mats under stronger salinities and/or more desiccated conditions, such as those of Lake 22. Our finding of such significant differences in two adjacent mat settings on the same island calls for great caution when studying sterols in microbialites or in modern microbial mats and making generalizations for the fossil record. Sterol preservation within microbial mats is a complex process that may be strongly influenced by environmental parameters. Therefore, palaeoenvironments must be thoroughly constrained if the presence, or absence, of

25 these compounds is interpreted in the study of ancient deposits.

5 Conclusion

The preservation of primary eukaryotic sterols and their progressive alteration was studied in a c. 1500 years old microbial mat from the hypersaline Lake 2 on Kiritimati. High $\delta^{13}C$ values of C_{31}-sterols and fatty acids suggest an autochthonous origin for these lipids. Total sterols decreased immediately below the uppermost layer, suggesting a major degradation of

30 these compounds within the mat. A different pattern was observed for unusual, isotopically heavy C_{31}-sterols (4α-methylgorgosterol and 4α-methylgorgostanol; $\delta^{13}C = -7.2$ ‰), which showed increasing abundances in the deeper mat layers as compared to the conventional C_{27}-C_{29} sterols. These C_{31} sterols may have partly derived from resting cells of

dinoflagellates, or their unusual side-chain might hamper degradation, which may have enhanced the resistance of these sterols against degradation. No significant 'trapping' of sterols into the mineral lattice occurred in this mat. Likewise, steroids were not sequestered into insoluble organic matter (as opposed to hopanoids). It is therefore suggested that the studied mat might have formed an effective filter against the preservation of sterols in the sedimentary record. The results

5   from this microbial mat, therefore, support the hypothesis of a 'mat-seal effect' describing the degradation of eukaryote-derived lipids in benthic microbial mats. Our results are markedly different from those recently obtained from another mat from Kiritimati Lake 22, where sterols showed no systematic decrease with depth, suggesting that the preservation of sterol carbon skeletons in that microbial mat did not suffer from a mat-seal effect. In that lake, an even higher salinity or temporal subaerial exposure may have hampered microbial metabolism and instead promoted sterol transformation rather than

10   degradation. The combined data show that sterol taphonomy may strongly vary between different mat systems, and even contrasting sterol degradation patterns may be expected in response to environmental conditions.

Code and data availability. Data can be found in the Supplement or can be requested from Yan Shen (yshen@gwdg.de).

Author contributions. YS had the main responsibility for analysing the data and writing the manuscript. JR and VT designed the project. JR conducted the field works, collected all the sample materials and participated in the writing process. VT contributed the conceptualisation of this work, participated in constructing the measurement setup and the writing process.
5 PSG had the main responsibility for the bulk data measurements, participated in the writing process. SWP participated in the interpretation of the data and the writing process. All the co-authors contributed to this work.

Competing interests. The authors declare that they have no conflict of interest.

Acknowledgements. We thank Prof. Dr. Gernot Arp and Dr. Martin Blumenberg for helpful information and constructive comments. Dr. Andreas Reimer is acknowledged for hydrochemical measurements. We are grateful that Dr. Jens. Dyckmans
10 analyse the compound-specific carbon isotopes. Dr. Pablo Suarez-Gonzalez acknowledges funding by a postdoctoral research fellowship of the Alexander von Humboldt Foundation. Wolfgang Dröse, Birgit Röring and Dorothea Hause-Reitner are kindly acknowledged for laboratory assistance. This research has received funding from the German Research Foundation (DFG, Project Re 665/18-2 and Research Unit 571 "Geobiology of Organo- and Biofilms").

References

Abed, R. M. M., Al-Thukair, A., and de Beer, D.: Bacterial diversity of a cyanobacterial mat degrading petroleum compounds at elevated salinities and temperatures, FEMS Microbiology Ecology, 57, 290–301, https://doi.org/10.1111/j.1574-6941.2006.00113.x, 2006.

5   Amo, M., Suzuki, N., Kawamura, H., Yamaguchi, A., Takano, Y., and Horiguchi, T.: Sterol composition of dinoflagellates: Different abundance and composition in heterotrophic species and resting cysts, Geochemical Journal, 44, 225–231, https://doi.org/10.2343/geochemj.1.0063, 2010.

Anbar, A. D. and Knoll, A. H.: Proterozoic ocean chemistry and evolution: A bioinorganic bridge?, Science, 297, 1137–1142, https://doi.org/10.1126/science.1069651, 2002.

10   Arp, G., Helms, G., Karlinska, K., Schumann, G., Reimer, A., Reitner, J., and Trichet, J.: Photosynthesis versus Exopolymer Degradation in the Formation of Microbialites on the Atoll of Kiritimati, Republic of Kiribati, Central Pacific, Geomicrobiology Journal, 29, 29–65, , https://doi.org/10.1080/01490451.2010.521436, 2012.

Arp, G., Reimer, A., and Reitner, J.: Calcification in cyanobacterial biofilms of alkaline salt lakes, European Journal of Phycology, 34, 393–403, https://doi.org/10.1080/09670269910001736452, 1999.

15   Atwood, A. R., Volkman, J. K., and Sachs, J. P.: Characterization of unusual sterols and long chain diols, triols, keto-ols and n-alkenols in El Junco Lake, Galápagos, Organic Geochemistry, 66, 80–89, https://doi.org/10.1016/j.orggeochem.2013.11.004, 2014.

Birgel, D., Thiel, V., Hinrichs, K.-U., Elvert, M., Campbell, K. A., Reitner, J., Farmer, J. D., and Peckmann, J.: Lipid biomarker patterns of methane-seep microbialites from the Mesozoic convergent margin of California, Organic
20   Geochemistry, 37, 1289–1302, https://doi.org/10.1016/j.orggeochem.2006.02.004, 2006.

Birk, J. J., Dippold, M., Wiesenberg, G. L. B., and Glaser, B.: Combined quantification of faecal sterols, stanols, stanones and bile acids in soils and terrestrial sediments by gas chromatography-mass spectrometry, Journal of chromatography. A, 1242, 1–10, https://doi.org/10.1016/j.chroma.2012.04.027, 2012.

Blumenberg, M., Thiel, V., and Reitner, J.: Organic matter preservation in the carbonate matrix of a recent microbial mat –
25   Is there a 'mat seal effect'?, Organic Geochemistry, 87, 25–34, https://doi.org/10.1016/j.orggeochem.2015.07.005, 2015.

Blumenberg, M., Thiel, V., Riegel, W., Kah, L. C., and Reitner, J.: Biomarkers of black shales formed by microbial mats, Late Mesoproterozoic (1.1Ga) Taoudeni Basin, Mauritania, Precambrian Research, 196-197, 113–127, https://doi.org/10.1016/j.precamres.2011.11.010, 2012.

Bolhuis, H., Cretoiu, M. S., and Stal, L. J.: Molecular ecology of microbial mats, FEMS Microbiology Ecology, 90, 335–
30   350, https://doi.org/10.1111/1574-6941.12408, 2014.

Brassell, S. C. and Eglinton, G.: Steroids and triterpenoids in deep sea sediments as environmental and diagenetic indicators, Advances in Organic Geochemistry 1981, 684–697, 1983.

Brocks, J. J., Jarrett, A. J. M., Sirantoine, E., Hallmann, C., Hoshino, Y., and Liyanage, T.: The rise of algae in Cryogenian oceans and the emergence of animals, Nature, 548, 578–581, https://doi.org/10.1038/nature23457, 2017.

Brocks, J. J. and Summons, R. E.: Sedimentary Hydrocarbons, Biomarkers for Early Life, Treatise on Geochemistry, 8, 63–115, https://doi.org/10.1016/B0-08-043751-6/08127-5, 2004.

5   Bühring, S. I., Smittenberg, R. H., Sachse, D., Lipp, J. S., Golubic, S., Sachs, J. P., Hinrichs, K. U., Summons, R. E., and (None): A hypersaline microbial mat from the Pacific Atoll Kiritimati: insights into composition and carbon fixation using biomarker analyses and a ^{13}C-labeling approach, Geobiology, 7, 308–323, https://doi.org/10.1111/j.1472-4669.2009.00198.x, 2009.

Close, H. G., Bovee, R., and Pearson, A.: Inverse carbon isotope patterns of lipids and kerogen record heterogeneous
10   primary biomass, Geobiology, 9, 250–265, https://doi.org/10.1111/j.1472-4669.2011.00273.x, 2011.

Decho, A. W.: Extracellular polymeric substances (EPS), Encyclopedia of Geobiology, 359–361, 2011.

Des Marais, D. J.: Biogeochemistry of hypersaline microbial mats illustrates the dynamics of modern microbial ecosystems and the early evolution of the biosphere, The Biological bulletin, 204, 160–167, https://doi.org/10.2307/1543552, 2003.

Dupraz, C., Pamela Reid, R., Braissant, O., Decho, A. W., Norman, R. S., and Visscher, P. T.: Processes of carbonate
15   precipitation   in   modern   microbial   mats,   Earth-Science   Reviews,   96,   141–162, https://doi.org/10.1016/j.earscirev.2008.10.005, 2009.

Dutkiewicz, A., Volk, H., Ridley, J., and George, S.: Biomarkers, brines, and oil in the Mesoproterozoic, Roper Superbasin, Australia, Geology, 31, 981–984, http://doi.org/10.1130/G19754.1, 2003.

Fowler, S. W. and Knauer, G. A.: Role of large particles in the transport of elements and organic compounds through the
20   oceanic water column, Progress in Oceanography, 16, 147–194, https://doi.org/10.1016/0079-6611(86)90032-7, 1986.

Gaskell, S. and Eglinton, G.: Sterols of a contemporary lacustrine sediment, Geochimica et Cosmochimica Acta, 40, 1221–1228, https://doi.org/10.1016/0016-7037(76)90157-5, 1976.

Gaskell, S. J. and Eglinton, G.: Rapid hydrogenation of sterols in a contemporary lacustrine sediment, Nature, 254, 209–211, https://doi.org/10.1038/254209b0, 1975.

25   Giner, J.-L., Faraldos, J. A., and Boyer, G. L.: Novel sterols of the toxic dinoflagellate *Karevia Brevis* (Dinophyceae): a defensive function for unusual marine sterols?, J Phycol, 39, 31–319, https://doi.org/10.1046/j.1529-8817.2003.01254.x, 2003.

Grimalt, J. O., de Wit, R., Teixidor, P., and Albaigés, J.: Lipid biogeochemistry of Phormidium and Microcoleus mats, Organic Geochemistry, 19, 509–530, https://doi.org/10.1016/0146-6380(92)90015-P, 1992.

30   Grotzinger, J. P. and Knoll, A. H.: Stromatolites in Precambrian carbonates: evolutionary mileposts or environmental dipsticks?, Annual review of earth and planetary sciences, 27, 313–358, https://doi.org/10.1146/annurev.earth.27.1.313, 1999.

Houle, H. M., Lopez, C. B., and Leblond, J. D.: Sterols of the Toxic Marine Dinoflagellate, *Pyrodinium bahamense*, The Journal of eukaryotic microbiology, 1–5, In Press. https://doi.org/10.1111/jeu.12684, 2018.

Ionescu, D., Spitzer, S., Reimer, A., Schneider, D., Daniel, R., Reitner, J., de Beer, D., and Arp, G.: Calcium dynamics in microbialite-forming exopolymer-rich mats on the atoll of Kiritimati, Republic of Kiribati, Central Pacific, Geobiology, 13, 170–180, https://doi.org/10.1111/gbi.12120, 2015.

Knoll, A. H., Summons, R. E., Waldbauer, J. R., and Zumberge, J. E.: The Geological Succession of Primary Producers in the Oceans, in: Evolution of Primary Producers in the Sea, Elsevier, 133–163, https://doi.org/10.1016/B978-012370518-1/50009-6, 2007.

Logan, G. A., Hayes, J. M., Hieshima, G. B., and Summons, R. E.: Terminal Proterozoic reorganization of biogeochemical cycles, Nature, 376, 53–56, https://doi.org/10.1038/376053a0, 1995.

Mattern, G., Albrecht, P., and Ourisson, G.: 4-Methyl-sterols and sterols in Messel Shale (Eocene), Chemical Communications, 1570–1571, https://doi.org/10.1039/C29700001570, 1970.

Nishimura, M.: Origin of stanols in young lacustrine sediments, Nature, 270, 711–712, https://doi.org/10.1038/270711a0, 1977.

O'Reilly, S. S., Mariotti, G., Winter, A. R., Newman, S. A., Matys, E. D., McDermott, F., Pruss, S. B., Bosak, T., Summons, R. E., and Klepac-Ceraj, V.: Molecular biosignatures reveal common benthic microbial sources of organic matter in ooids and grapestones from Pigeon Cay, The Bahamas, Geobiology, 15, 112–130, https://doi.org/10.1111/gbi.12196, 2017.

Otto, A. and Simpson, M. J.: Degradation and Preservation of Vascular Plant-derived Biomarkers in Grassland and Forest Soils from Western Canada, Biogeochemistry, 74, 377–409, https://doi.org/10.1007/s10533-004-5834-8, 2005.

Pagès, A., Grice, K., Ertefai, T., Skrzypek, G., Jahnert, R., and Greenwood, P.: Organic geochemical studies of modern microbial mats from Shark Bay: Part I: Influence of depth and salinity on lipid biomarkers and their isotopic signatures, Geobiology, 12, 469–487, https://doi.org/10.1111/gbi.12094, 2014.

Pawlowska, M. M., Butterfield, N. J., and Brocks, J. J.: Lipid taphonomy in the Proterozoic and the effect of microbial mats on biomarker preservation, Geology, 41, 103–106, https://doi.org/10.1130/G33525.1, 2013.

Peckmann, J. and Thiel, V.: Carbon cycling at ancient methane–seeps, Chemical Geology, 205, 443–467, https://doi.org/10.1016/j.chemgeo.2003.12.025, 2004.

Rampen, S. W., Abbas, B. A., Schouten, S., and Sinninghe Damsté, J. S.: A comprehensive study of sterols in marine diatoms (Bacillariophyta): Implications for their use as tracers for diatom productivity, Limnol. Oceanogr., 55, 91–105, https://doi.org/10.4319/lo.2010.55.1.0091, 2010.

Rampen, S. W., Schouten, S., Hopmans, E. C., Abbas, B., Noordeloos, A. A.M., van Bleijswijk, J. D.L., Geenevasen, J. A.J., and Sinninghe Damsté, J. S.: Diatoms as a source for 4-desmethyl-23,24-dimethyl steroids in sediments and petroleum, Geochimica et Cosmochimica Acta, 73, 377–387, https://doi.org/10.1016/j.gca.2008.10.024, 2009.

Reitner, J. and Thiel, V. (Eds): Encoclopedia of Geobiology, Springer, 1–956, 2011.

Riding, R.: The Nature of Stromatolites: 3,500 Million Years of History and a Century of Research, in: Advances in Stromatolite Geobiology, Reitner, J., Quéric, N.-V., Arp, G. (Eds.), Lecture Notes in Earth Sciences, Springer Berlin Heidelberg, Berlin, Heidelberg, 29–74, https://doi.org/ 10.1007/978-3-642-10415-2_3, 2011.

Robinson, N., Cranwell, P. A., Finlay, B. J., and Eglinton, G.: Lipids of aquatic organisms as potential contributors to
5   lacustrine sediments, Organic Geochemistry, 6, 143–152, https://doi.org/10.1016/0146-6380(84)90035-4, 1984.

Rosenfeld, R. S. and Hellman, L.: Reduction and esterification of cholesterol and sitosterol by homogenates of feces, Journal of Lipid Research, 12, 192–197, 1971.

Saenger, C., Miller, M., Smittenberg, R. H., and Sachs, J. P.: A physico-chemical survey of inland lakes and saline ponds: Christmas Island (Kiritimati) and Washington (Teraina) Islands, Republic of Kiribati, Saline systems, 2, 1–15,
10   https://doi.org/10.1186/1746-1448-2-8, 2006.

Scherf, A.-K. and Rullkötter, J.: Biogeochemistry of high salinity microbial mats – Part 1: Lipid composition of microbial mats across intertidal flats of Abu Dhabi, United Arab Emirates, Organic Geochemistry, 40, 1018–1028, https://doi.org/10.1016/j.orggeochem.2009.04.002, 2009.

Schneider, D., Arp, G., Reimer, A., Reitner, J., Daniel, R., and Balcazar, J. L.: Phylogenetic Analysis of a Microbialite-
15   Forming Microbial Mat from a Hypersaline Lake of the Kiritimati Atoll, Central Pacific, PLoS ONE, 8, e66662, https://doi.org/10.1371/journal.pone.0066662, 2013.

Schouten, S., Hartgers, W. A., Lopez, J. F., Grimalt, J. O., and Sinninghe Damsté, J. S.: A molecular isotopic study of ^{13}C-enriched organic matter in evaporitic deposits: recognition of CO_2-limited ecosystems, Organic Geochemistry, 32, 277–286, https://doi.org/10.1016/S0146-6380(00)00177-7, 2001.

20 Shen, Y., Thiel, V., Duda, J.-P., and Reitner, J.: Tracing the fate of steroids through a hypersaline microbial mat (Kiritimati, Kiribati/Central Pacific), Geobiology, 16, 307–318, https://doi.org/10.1111/gbi.12279, 2018a.

Shen, Y., Suarez-Gonzalez, P., Thiel V., Blumenberg, M., Reitner, J.: Different modes of calcification control the preservation of organic matter in a recent microbial mat. AGU Fall Meeting, Washington, D.C., USA, 10-14 December 2018, B43H-2952, 2018b.

25 Słowakiewicz, M., Whitaker, F., Thomas, L., Tucker, M. E., Zheng, Y., Gedl, P., and Pancost, R. D.: Biogeochemistry of intertidal microbial mats from Qatar: New insights from organic matter characterisation, Organic Geochemistry, 102, 14–29, https://doi.org/10.1016/j.orggeochem.2016.09.006, 2016.

Smrzka, D., Zwicker, J., Kolonic, S., Birgel, D., Little, C. T.S., Marzouk, A. M., Chellai, E. H., Wagner, T., and Peckmann, J.: Methane seepage in a Cretaceous greenhouse world recorded by an unusual carbonate deposit from the Tarfaya
30   Basin, Morocco, Depositional Rec, 3, 4–37, https://doi.org/10.1002/dep2.24, 2017.

Summons, R. E., Bird, L. R., Gillespie, A. L., Pruss, S. B., Roberts, M., and Sessions, A. L.: Lipid biomarkers in ooids from different locations and ages: evidence for a common bacterial flora, Geobiology, 11, 420–436, https://doi.org/10.1111/gbi.12047, 2013.

Summons, R. E., Powell, T. G., and Boreham, C. J.: Petroleum geology and geochemistry of the middle Proterozoic McArthur Basin, Northern Australia: III. Composition of extractable hydrocarbons, Geochimica et Cosmochimica Acta, 52, 1747–1763, https://doi.org/10.1016/0016-7037(88)90001-4, 1988.

Thiel, V., Peckmann, J., Richnow, H. H., Luth, U., Reitner, J., and Michaelis, W.: Molecular signals for anaerobic methane oxidation in Black Sea seep carbonates and a microbial mat, Marine Chemistry, 73, 97–112, https://doi.org/10.1016/S0304-4203(00)00099-2, 2001.

Thiel, V., Peckmann, J., Seifert, R., Wehrung, P., Reitner, J., and Michaelis, W.: Highly isotopically depleted isoprenoids: Molecular markers for ancient methane venting, Geochimica et Cosmochimica Acta, 63, 3959–3966, https://doi.org/10.1016/S0016-7037(99)00177-5, 1999.

Trichet, J., Défarge, C., Tribble, J., Tribble, G., and Sansone, F.: Christmas Island lagoonal lakes, models for the deposition of carbonate-evaporite-organic laminated sediments, Sedimentary Geology, 140, 177–189, https://doi.org/10.1016/S0037-0738(00)00177-9, 2001.

Valencia, M.: Christmas Island (Pacific ocean): Reconnaissance geologic observations, Atoll Research Bulletin, https://doi.org/10.5479/si.00775630.197.1, 1977.

van Bergen, P. F., Bull, I. D., Poulton, P. R., and Evershed, R. P.: Organic geochemical studies of soils from the Rothamsted classical experiments-I. Total lipid extracts, solvent insoluble residues and humic acids from Broadbalk Wilderness, Organic Geochemistry, 26, 117–135, https://doi.org/10.1016/S0146-6380(96)00134-9, 1997.

van Gemerden, H.: Microbial mats: A joint venture, Marine Geology, 113, 3–25, https://doi.org/10.1016/0025-3227(93)90146-M, 1993.

Volkman, J. K.: A review of sterol markers for marine and terrigenous organic matter, Organic Geochemistry, 9, 83–99, https://doi.org/10.1016/0146-6380(86)90089-6, 1986.

Volkman, J. K.: Sterols in microorganisms, Appl Microbiol Biotechnol, 60, 495–506, https://doi.org/10.1007/s00253-002-1172-8, 2003.

Volkman, J. K.: Sterols and other triterpenoids: Source specificity and evolution of biosynthetic pathways, Organic Geochemistry, 36, 139–159, https://doi.org/10.1016/j.orggeochem.2004.06.013, 2005.

Wakeham, S. G.: Reduction of stenols to stanols in particulate matter at oxic-anoxic boundaries in sea water, Nature, 342, 787–790, https://doi.org/10.1038/342787a0, 1989.

Walter, M. R.: Stromatolites, Developments in Sedimentology, 20, Elsevier Scientific Pub. Co, Amsterdam, New York, 1976.

Ward, D. M. and Brock, T. D.: Hydrocarbon biodegradation in hypersaline environments, Applied and Environmental Microbiology, 35, 353–359, 1978.

Wingender, J., Neu, T. R., and Flemming, H.-C. (Eds): Microbial Extracellular Polymeric Substances; Characterization, Structure, and Function. Springer, Berlin, Heidelberg, Germany, 258 p, 1999.
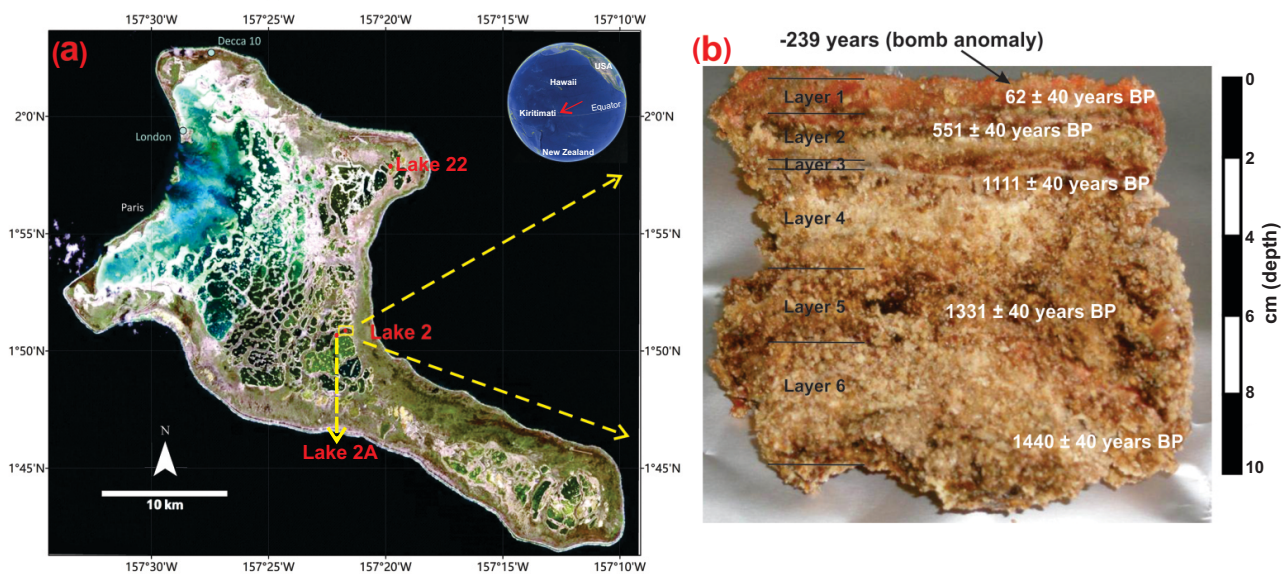
Figure 1. (a) Location of Kiritimati atoll in the Pacific Ocean and its satellite image showing reticulate distribution pattern of the lakes (red

dots: Lake 2 studied in this work; Lake 2A and 22 previously studied by Bühring et al., 2009 and Shen et al., 2018a); (b) the microbial mat

sample from Lake 2 studied in this work (^{14}C data from Blumenberg et al., 2015).
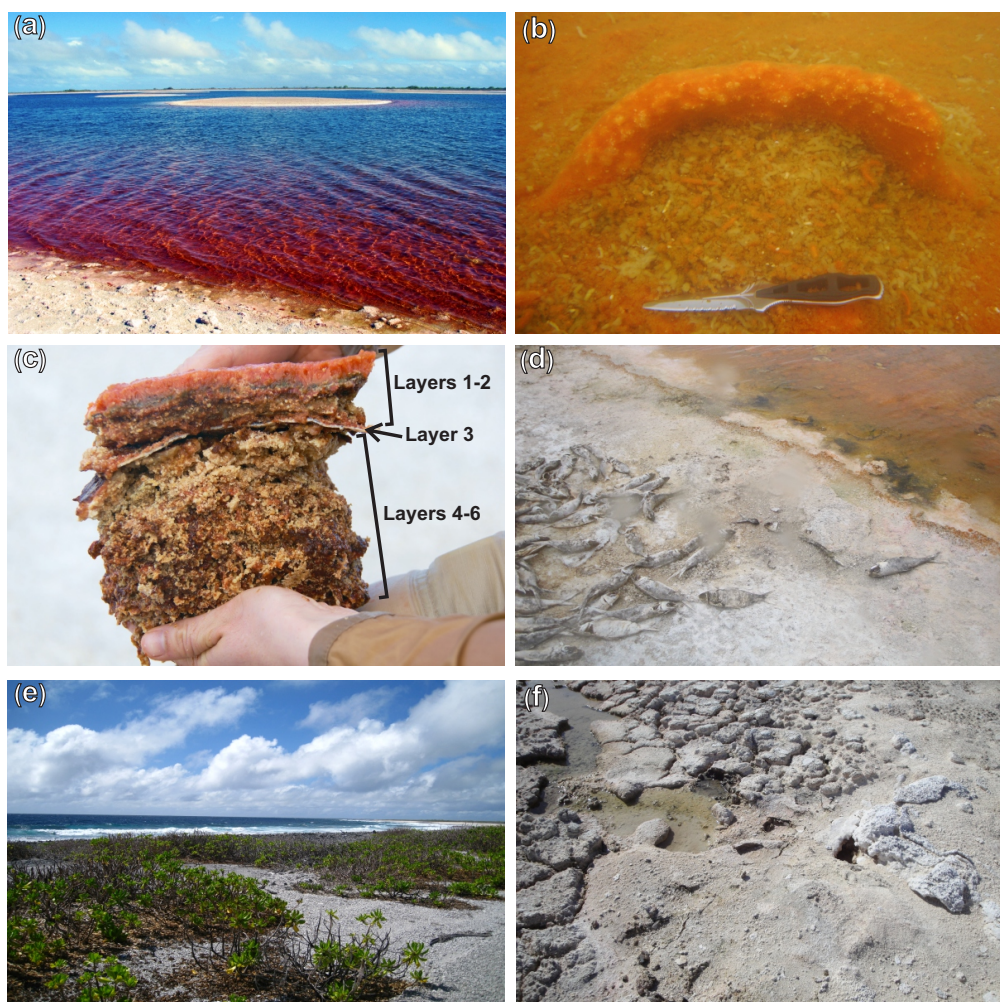
Figure 2. Field images: (a) general view of hypersaline Lake 2 in Kiritimati; (b) underwater photograph showing an example of a currently-active, orange-coloured microbial mat at the bottom of the lake; (c) the microbial mat sampled for this study, with clear colour-zonation; note the whitish mineral crust (Layer 3) separating the upper younger growth phase from the older, more mineralized layers; (d) lake shore showing dead fish; (e) vegetation around the lake area; (f) sampling site for hypersaline Lake 22 mat (Shen et al., 2018a)
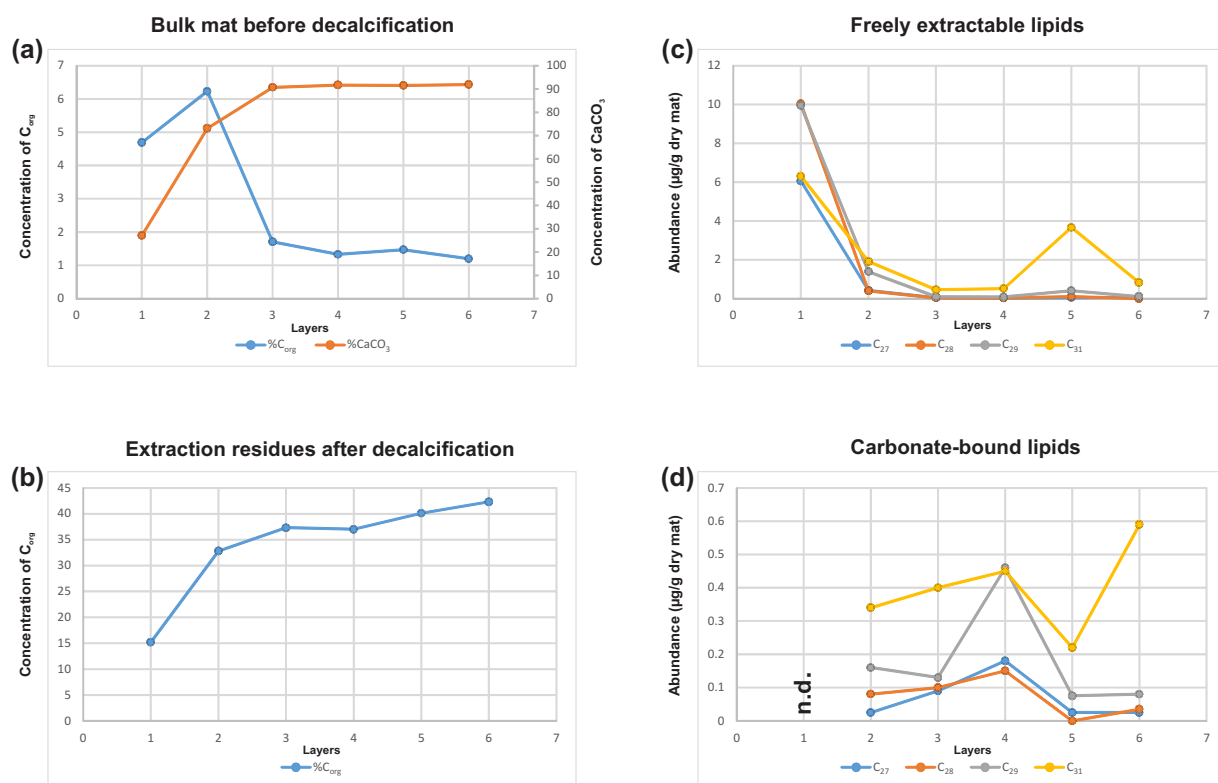
Figure 3. (a) C_{org} and $CaCO_3$ contents of the bulk mat ($\%_{wt}$); (b) C_{org} content of the extraction residues after decalcification ($\%_{wt}$); (c) Distribution of C_{27}- vs. C_{28}- vs. C_{29}- vs. C_{31}- sterols in the freely extractable lipids (µg/g dry mat); (d) Distribution of C_{27}- vs. C_{28}- vs. C_{29}- vs. C_{31}- sterols in the carbonate-bound lipids of the microbial mat (µg/g dry mat).
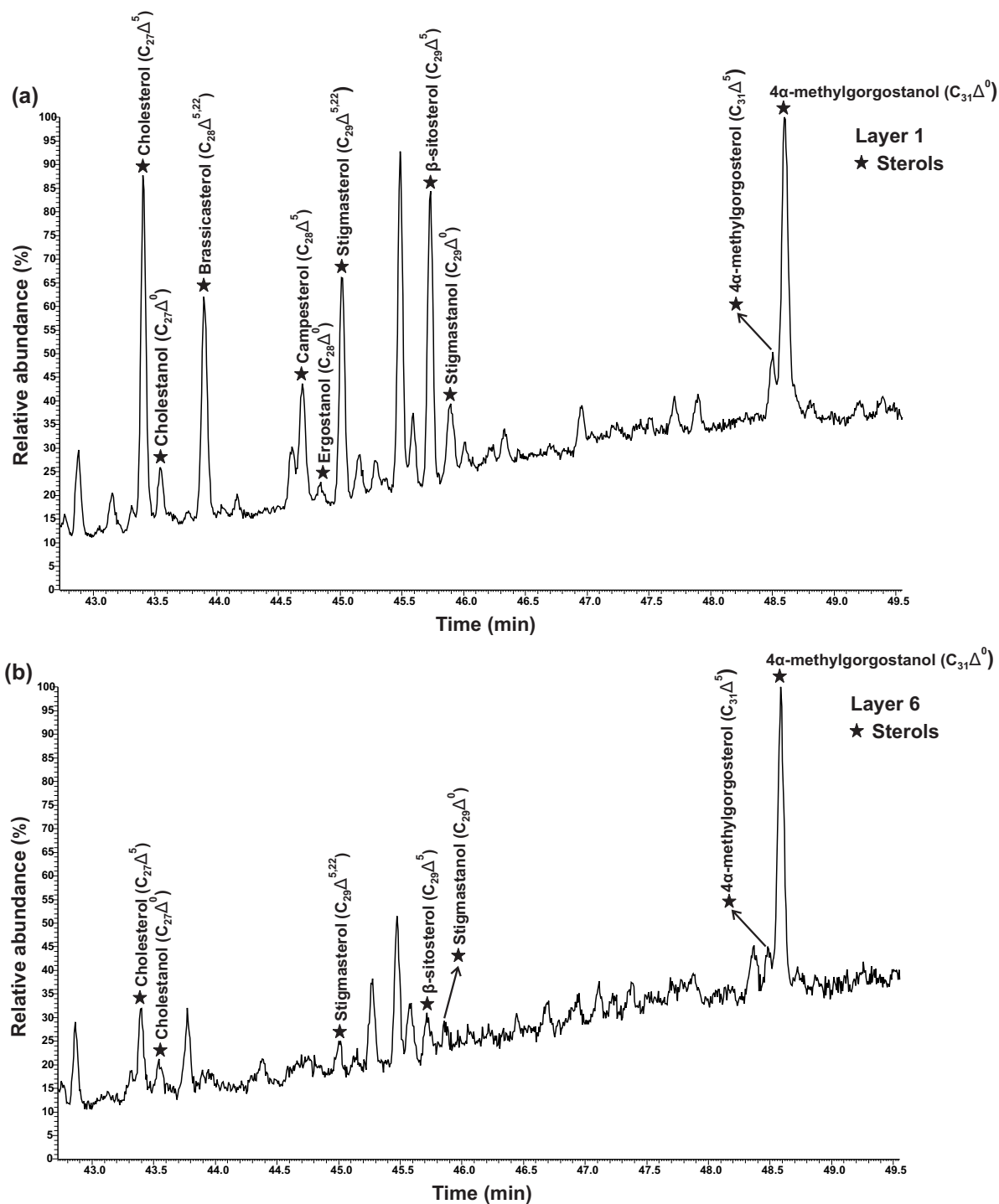
Figure 4. Partial GC-MS chromatograms (total ion current) showing the distributions of freely extractable sterols

(TMS-derivatives) in (a) layer 1, and (b) layer 6 of the microbial mat.
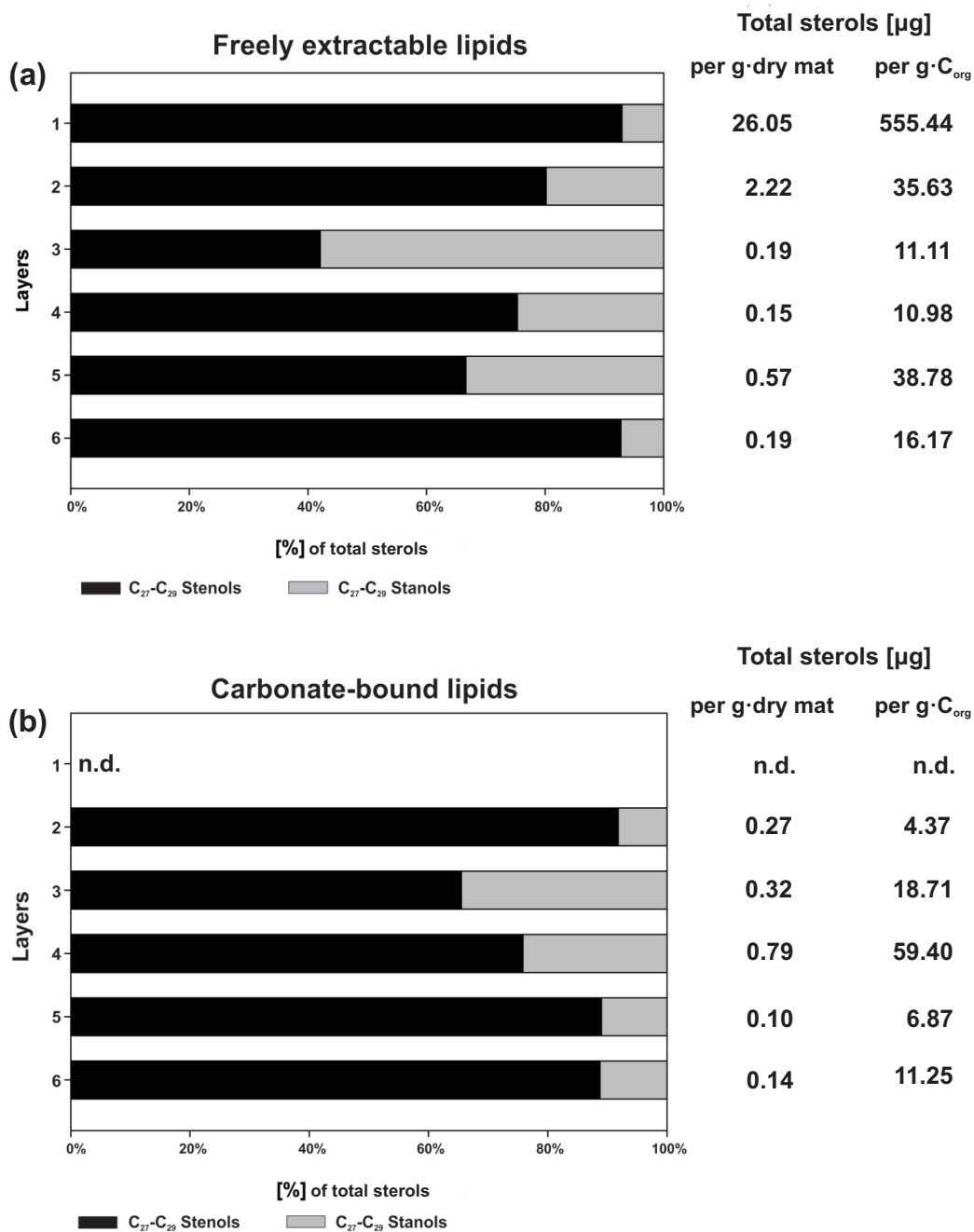
Figure 5. Distributions and concentrations of C_{27}-C_{29} sterols in the microbial mat layers, (a) freely extractable lipids, and (b) carbonate-bound lipids.
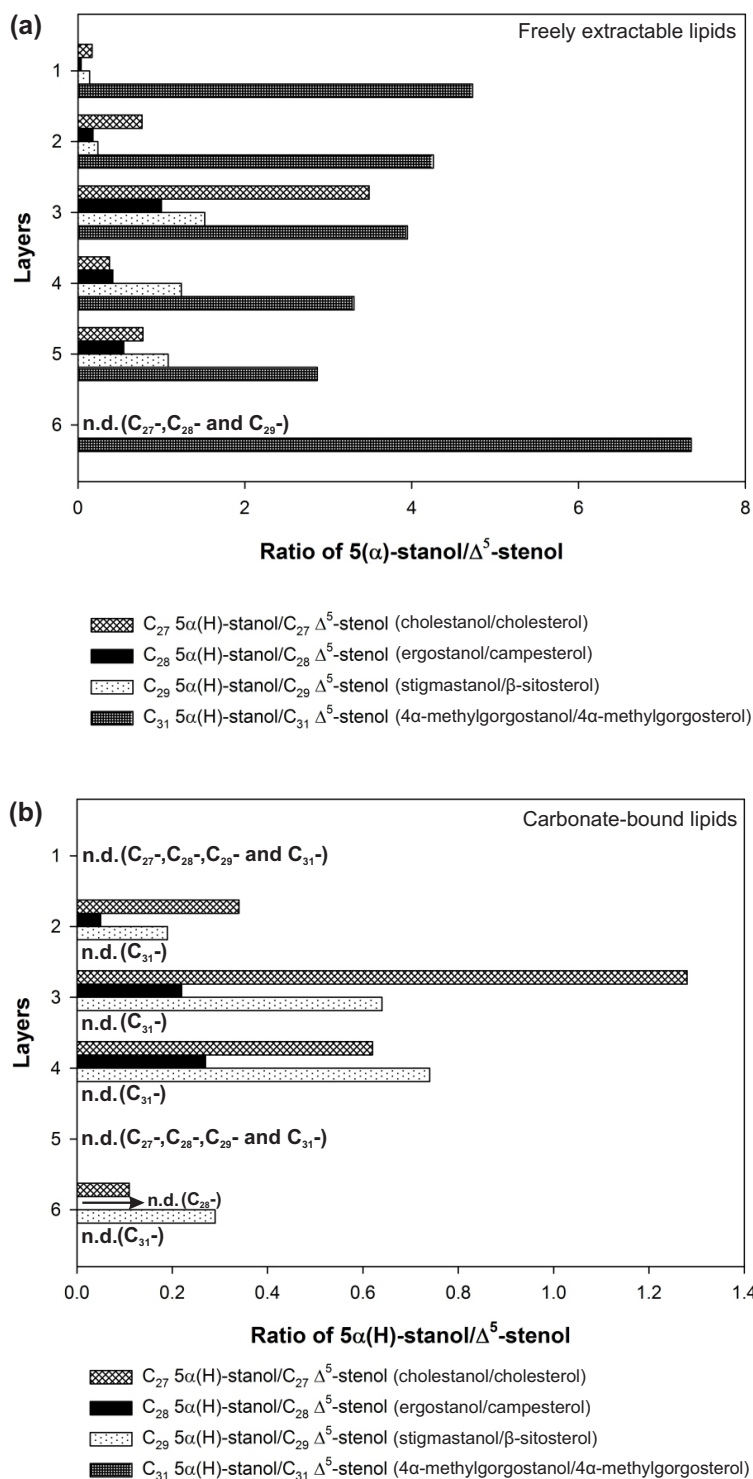
Figure 6. Stanol/stenol ratios for the microbial mat layers, (a) freely extractable lipids, and (b) carbonate-bound lipids.

Table 1a. Bulk geochemical data for the microbial mat (original mat layers before decalcification)

Layers	C_{tot} (%)	C_{org} (%)	C_{carb} (%)	$CaCO_3$ (%)	N_{tot} (%)	S_{tot} (%)	C_{org}/N	C_{org}/S
1	7.94	4.69	3.25	27.10	0.41	9.78	11.40	0.50
2	15.00	6.23	8.77	73.10	0.74	1.21	8.40	5.20
3	12.59	1.71	10.88	90.70	0.16	0.33	10.50	5.10
4	12.33	1.33	11.00	91.70	0.19	0.49	7.00	2.70
5	12.45	1.47	10.98	91.50	0.20	0.52	7.30	2.80
6	12.23	1.20	11.03	91.90	0.14	0.48	8.50	2.50

Table 1b. Bulk geochemical data for the microbial mat (extraction residues after decalcification; modified after Blumenberg et al., 2015)

Layers	C_{org} (%)	N_{tot} (%)	S_{tot} (%)	C_{org}/N	C_{org}/S
1	15.2	1.9	10.4	7.9	1.5
2	32.8	4.9	2.9	6.7	11.4
3	37.3	5.6	4.6	6.7	8.2
4	37.0	6.2	2.6	6.0	14.4
5	40.1	6.7	2.0	6.0	20.3
6	42.3	6.6	2.0	6.4	21.4

Table2a. Concentrations of sterols in the freely extractable lipids of the microbial mat layers. SD indicate mean value of standard deviation (µg/g dry mat; n.d. = not detected).

Compound / Layers	Cholesterol Cholest-5-en-3β-ol	Cholestanol 5α-cholestan-3β-ol	Brassicasterol 24-methylcholesta-5,22-dien-3β-ol	Campesterol 24-methylcholest-5-en-3β-ol	Ergostanol 5α-24-methylcholestan-3β-ol	Stigmasterol 24-ethylcholesta-5,22-dien-3β-ol	β-sitosterol 24-ethylcholest-5-en-3β-ol	Stigmastanol 5α-24-ethylcholestan-3β-ol	4α-methylgorgosterol 22,23-methylene-4α,23,24-trimethylcholest-5-en-3β-ol	4α-methylgorgostanol 22,23-methylene-4α,23,24-trimethylcholestan-3β-ol
SD	28.4%	41.7%	12.31%	10.7%	28.3%	20.0%	13.2%	27.7%	41.3%	41.6%
1	5.20	0.86	4.93	4.91	0.20	3.74	5.44	0.77	1.10	5.21
2	0.24	0.19	n.d.	0.34	0.06	0.43	0.77	0.19	0.36	1.55
3	0.01	0.04	n.d.	0.02	0.02	0.02	0.03	0.05	0.09	0.37
4	0.02	<0.01	n.d.	0.02	0.01	0.05	0.02	0.02	0.12	0.40
5	0.03	0.02	n.d.	0.07	0.04	0.16	0.12	0.13	0.95	2.72
6	0.08	<0.01	n.d.	n.d.	n.d.	0.08	0.02	0.01	0.10	0.73

Table 2b. Concentrations of sterols in the carbonate-bound lipids of the microbial mat layers. SD indicate mean value of standard deviation (µg/g dry mat; n.d. = not detected; dashes indicate SD are not applicable).

Trivial names Compound \ Layers	Cholesterol Cholest-5-en-3β-ol	Cholestanol 5α-cholestan-3β-ol	Brassicasterol 24-methylcholesta-5,22-dien-3β-ol	Campesterol 24-methylcholest-5-en-3β-ol	Ergostanol 5α-24-methylcholestan-3β-ol	Stigmasterol 24-ethylcholesta-5,22-dien-3β-ol	β-sitosterol 24-ethylcholest-5-en-3β-ol	Stigmastanol 5α-24-ethylcholestan-3β-ol	4α-methylgorgosterol 22,23-methylene-4α,23,24-trimethylcholest-5-en-3β-ol	4α-methylgorgostanol 22,23-methylene-4α,23,24-trimethylcholestan-3β-ol
SD	24.0%	47.6%	—	—	—	—	24.8%	40.2%	—	—
1	n.d.	n.d.	n.d.	n.d.	n.d.	n.d.	n.d.	n.d.	n.d.	n.d.
2	0.02	<0.01	n.d.	0.08	<0.01	0.08	0.07	0.01	n.d.	0.34
3	0.04	0.05	n.d.	0.08	0.02	0.03	0.06	0.04	n.d.	0.40
4	0.11	0.07	n.d.	0.12	0.03	0.25	0.12	0.09	n.d.	0.45
5	0.02	<0.01	n.d.	n.d.	n.d.	0.06	0.01	<0.01	n.d.	0.22
6	0.02	<0.01	n.d.	0.03	<0.01	0.04	0.03	0.01	n.d.	0.59

Table 3 Stanol/stenol ratios in the freely extractable lipids and carbonate-bound lipids for the microbial mat layers (n.d. = not determined, due to very low concentration of sterols).

Layer	stanol/stenol (Δ^0/Δ^5) in Free lipids				stanol/stenol (Δ^0/Δ^5) in carbonate-bound			
	C_{27}	C_{28}	C_{29}	C_{31}	C_{27}	C_{28}	C_{29}	C_{31}
1	0.17	0.04	0.14	4.73	n.d.	n.d.	n.d.	n.d.
2	0.77	0.18	0.24	4.26	0.34	0.05	0.19	n.d.
3	3.49	1.00	1.52	3.95	1.28	0.22	0.64	n.d.
4	0.38	0.42	1.24	3.31	0.62	0.27	0.74	n.d.
5	0.78	0.55	1.08	2.87	n.d.	n.d.	n.d.	n.d.
6	n.d.	n.d.	n.d.	7.35	0.11	n.d.	0.29	n.d.